

Thickness Identification of Tunnel Lining Structure by Time–Energy Density Analysis based on Wavelet Transform

Sheng Zhang^{1,2*}, Wenchao He³, Yongsuo Li¹ and Yuchi Zou¹

¹School of Civil Engineering, Hunan City University, Yiyang 413000, China

²Smart Materials and Structures Laboratory, Department of Mechanical Engineering, University of Houston, Houston, TX 77204, USA

³School of Civil Engineering, Changsha University of Science & Technology, Changsha 410114, China

Received 27 April 2019; Accepted 14 August 2019

Abstract

The concrete thickness of the tunnel lining structure and cover depth is insufficient. Such condition seriously affects the safety and stability of the lining structure. The lining structure thickness is difficult to identify using radar profile horizon tracing method because of the strong interference of steel bars to electromagnetic wave propagation. To explore the reflection characteristics of electromagnetic wave signals at the interface between deep concrete and surrounding rock, a time–energy density analysis based on wavelet transform (TEDAWT) was proposed in this study. Ground–penetrating radar (GPR) forward modelling of the lining structure with different thicknesses of plain and reinforced concrete was carried out by using different central frequencies, namely, 1600 and 900 MHz, respectively. On this basis, the GPR detection signals for the plain and reinforced concrete lining structures were analyzed by employing the TEDAWT method. The feasibility of the TEDAWT method in GPR quantitative identification was verified using physical experiment. Results demonstrate that the identification accuracy of different thicknesses of plain and reinforced concrete structure is high regardless of the method used in either forward modelling or physical experiment, and the relative error is less than 5%. In the identification of concrete cover depth, the resolution of a 1600 MHz antenna is higher than that of a 900 MHz antenna, and the relative error is also less than 5%. The results indicate the application potential of the proposed method for quantitative identification of tunnel lining thickness by non–destructive testing. The proposed method provides not only the thickness distribution of the plain concrete structure but also the distribution of the reinforced concrete structure and concrete cover depth compared with traditional radar profile horizon tracing method.

Keywords: Tunnel engineering, Lining structure, GPR, TEDAWT, Finite–difference time–domain method

1. Introduction

Since the Belt and Road Initiative was first proposed in 2013, infrastructural connectivity has become a priority for implementing the initiative. Tunnels are one of the most important passageways, critical nodes, and key control projects in traffic infrastructural construction. At the end of 2018, China's tunnel construction included railway, highway, and urban rail transit tunnels, which had a total length of 36,103 km. Currently, 20,000 km of various types of tunnels is under construction, and another 20,000 km of tunnels will be constructed in the future [1]. In the process of tunnel construction, the cavity and void easily develop between the surrounding rock and the lining structure due to various problems, such as bad effect in rock blasting, non–standard construction, and insufficient pressure of pumping concrete; such phenomenon leads to the insufficient concrete lining thickness [2]. A slightly insufficient concrete lining thickness causes the settlement of tunnel lining and affects the construction boundary. When the concrete lining thickness is seriously insufficient, it leads to fracture, collapse, and other accidents of the lining structure; such condition greatly reduces the bearing capacity of the lining

structure and affects the normal use of tunnel in operation. The concrete cover depth is another important factor affecting the durability and corrosion resistance of the tunnel lining structure [3–4]. When the actual thickness of the concrete cover depth cannot meet the design requirements, the steel bar is easily eroded by harmful substances. The corrosion and deterioration of the steel bar seriously affect and threaten the safety and stability of the entire reinforced concrete structure. Therefore, the thickness of the lining structure and concrete cover depth must be checked.

At present, the methods commonly used to measure lining structure thickness include embedded steel bar, drilling, coring, profiler, and ground–penetrating radar (GPR) methods [5]. Among them, GPR has been widely used in the detection of lining structure thickness due to its high detection accuracy, non–destructive testing, intuitive results, and flexible operation [6]. In the field detection process of GPR, the original signal is often interfered by a complex environment. Accordingly, the original signal needs to be processed by advanced signal analysis method before being interpreted. In recent years, with the technical breakthrough in signal analysis and processing, the wavelet time–frequency analysis method has been developed; this method has a good interpretation ability in different aspects, such as signal denoising, feature extraction, spectrum analysis, and image recognition [7]. However, when the thickness of the reinforced concrete lining is identified, the

*E-mail address: zhangsheng040331@163.com

ISSN: 1791-2377 © 2019 School of Science, IHU. All rights reserved.

doi:10.25103/jestr.124.04

electromagnetic wave energy decays quickly due to the strong interference of steel bars on the electromagnetic wave signal. This process generates weak reflected signal at the interface between deep reinforced concrete and surrounding rock. Consequently, the thickness of the reinforced concrete lining structure is difficult to obtain. Thus, the following problems need to be solved in the application of wavelet theory to GPR signal processing: how to enhance the effective characteristics of weak signals and how to improve the accuracy of GPR signal analysis.

According to the features of GPR emission wavelet, a wavelet basis with high fit to GPR emission wavelet was constructed in the present study. On this basis, a time–energy density analysis based on wavelet transform (TEDAWT) was proposed and applied to quantitatively identify plain and reinforced concrete lining structures in the GPR forward modelling and physical experiment. Such task was carried out to provide technical support for the identification of the lining structure thickness and concrete cover depth.

2. State of the Art

At present, several quality defects, such as insufficient lining thickness, cavities, and non–compactness, are present in tunnels. The cause of these defects needs to be determined before they can be maintained or repaired. Similar to “observation, listening, interrogation, and pulse–taking” and “prescribing medicine for the defect” in clinics, the detection and diagnosis of tunnel lining quality defects involve comprehensive judgment. Since the first international seminar on GPR was held in Georgia, USA in 1986, a series of seminars on GPR has been held worldwide every two years for nearly 30 years. This fact shows that GPR has become a powerful tool for non–destructive testing of reinforced concrete structural defects and has played an important role in civil engineering fields, such as buildings, roads, bridges, tunnels, and geotechnical engineering [8–10]. As the electromagnetic waves are transmitted from air (or the second lining) to the second lining (or the first lining), the Fresnel reflective coefficient is negative. According to the amplitude of one–dimensional waveform in GPR time profile images, the thickness of the lining structure can be determined by calculating the positive or negative Fresnel reflection coefficient; however, GPR cannot recognize the reflection signal under the interference of steel bars [11]. A method to estimate the lining structure thickness was proposed on the basis of the reflection coefficient spectrum [12]. However, the GPR signal was treated as a simple stationary signal processing due to the limitation of spectral analytical theory. GPR forward modelling is the basis of radar image interpretation. Interpreters know the map characteristics of GPR forward modelling to clearly explain the tunnel lining defects [13–14]. Giannopoulos et al. conducted GPR two–dimensional forward modelling of lining cavities and summarized the characteristics of GPR detection response of lining cavities [15]. The forward modelling of lining defects is relatively simple, but the causes of these defects are complex. The law of electromagnetic wave propagation must be further studied according to the field defects. The Medway tunnel was completed in 1996. To know more about the detailed design of lining structure, Alani et al. used two sets of antenna systems with different frequencies (900 MHz and 2 GHz GPR) to detect the location and spacing of steel bars in the structural details [16]. The reflection of municipal pipelines

and other buried objects on the GPR time profile were generally hyperbolic. To obtain the shape characteristics of hyperbolas, Maas et al. developed a method for automatically locating reflected hyperbolas in GPR data [17]. Mechbal et al. used GPR data as a way to estimate the radius of steel bar and determined the wave velocity and coordinate of hyperbolic vertex according to hyperbolic trajectory and diffraction amplitude [18]. The traditional GPR interpretation method requires a large amount of labor and time. In addition, the target echo signal is seriously affected by the repeated reflection of the steel bar. Xie et al. proposed a new method to automatically identify the cavities’ GPR image of the reinforced concrete structure; they used the predictive deconvolution method to suppress multiple waves and obtained good results [19]. Jiang et al. proposed a quantitative system for health inspection and evaluation of the tunnel lining to ensure safety of the lining structure; such approach could effectively extract cracks and accurately evaluate the tunnel lining conditions [20]. On the basis of the grouting effect detected by the GPR image of Nanchang Metro Line 1, Yu et al. determined the thickness and distribution of grouting layer and obtained the GPR image features, such as gaps and cracks [21]. To ensure safety and quality service to passengers, Llanca et al. established an expert diagnosis system by combining qualitative and quantitative methods to make up for the shortcomings of visual inspections [22]. Taking Damashan tunnel in Fujian province as an example, Xiang et al. evaluated the condition of the lining structure by combining GPR and finite–difference time–domain (FDTD) technology and showed that the average qualified rate of lining thickness was 79.87% of the design parameters [23]. To ensure that GPR satisfies the requirements of lining defect investigation and regular inspection, Zan et al. developed a new method with remote detection (vehicle–mounted GPR), which provided a fast, interference–free method for periodic inspections and health assessments of existing tunnels [24]. Cui et al. extracted target echo reflected wave images from a large number of GPR measured data to establish a template database and matched the detected features and features in the template database with fuzzy logic algorithm to achieve automatic identification [25]. Baryshnikov and Lalagüe et al. studied the differences of detection accuracy of defects under different detection parameters by analyzing various types of reflected wave signals of tunnel defects; they also proposed a set of complete optimization rules of detection parameters [26–27]. Zhang et al. examined and counted the lining structures of more than 100 railway tunnels and obtained the contact state and distribution law behind tunnel lining, but they did not formulate an effective theoretical method [28]. The above–mentioned research results are mainly based on the non–destructive detection technology of GPR for tunnel lining quality defects. The interpretation of GPR data is still in the qualitative state on the basis of experience, and accurate quantitative interpretation results is difficult to obtain. When conducting forward modelling or physical experiment for lining quality defects, only simple simulation is carried out for common problems, without in–depth analysis of GPR feature signals. Therefore, a method of quantitative identification of concrete structural thickness under the interference of steel bar is urgently needed to improve the accuracy of GPR lining quality detection. In the present study, the FDTD method and indoor physical experiment were combined to carry out the non–destructive detection of tunnel lining concrete thickness, including concrete cover depth. The TEDAWT method was used to

quantitatively analyze the response characteristic signals of GPR of plain and reinforced concrete lining structures. Such method was also utilized to improve the identification accuracy of the thickness of concrete lining structure under the interference of steel bars, so as to provide guidance and reference for the interpretation of GPR image characteristics of tunnel lining.

The remainder of this study is organized as follows: The third section describes the principle of the FDTD method, constructs the forward model of plain and reinforced concrete lining structures, and analyzes the forward modelling response characteristics of concrete with different thicknesses by using the TEDAWT method. The fourth section introduces the physical experiment scheme according to the forward modelling results. Different central frequencies, namely, 1600 and 900 MHz, were adopted to collect data from the physical experiment. The thickness of plain and reinforced concrete lining and the concrete cover depth were obtained using the TEDAWT method. The last section provides the conclusions.

3. Methodology

3.1 FDTD method

The GPR forward modelling is the foundation of the interpretation of radar images. The interpreters should understand the propagation law and spectral characteristics of electromagnetic waves in the tunnel lining structure to clearly grasp and quantitatively interpret the GPR detection signals. The FDTD method has become the main method of GPR forward modelling because of its small storage space and high computational efficiency [29–30].

In the passive field, the two curls of Maxwell equation can be expressed as follows:

$$\begin{cases} \nabla \times H = \varepsilon \frac{\partial E}{\partial t} + \sigma E \\ \nabla \times E = -\mu \frac{\partial H}{\partial t} - \sigma_m H \end{cases} \quad (1)$$

where H is the intensity of magnetic field (A/m), E is the intensity of electric field (V/m), ε is the dielectric constant of the medium, σ is the electrical conductivity (S/m), t is time (s), μ is the relative permeability (H/m), and σ_m is equivalent permeability (w/m).

The FDTD method adopts the central difference form of the second order accuracy to convert the two curls in Maxwell equation from differential into difference. The electric and magnetic fields are sampled alternately in time sequence, with half time step difference between them. Therefore, the FDTD equation of two-dimensional electromagnetic wave can be expressed as follows:

$$\begin{aligned} E_x^{n+1}(i, j) &= CA \times E_x^n(i, j) + \\ &CB \times \frac{H_y^{n+1/2}(i+1/2, j) - H_y^{n+1/2}(i-1/2, j)}{\Delta x} - \\ &CB \times \frac{H_x^{n+1/2}(i, j+1/2) - H_x^{n+1/2}(i, j-1/2)}{\Delta y} \end{aligned} \quad (2)$$

$$\begin{aligned} H_x^{n+1/2}(i, j+1/2) &= CP \times H_x^{n-1/2}(i, j+1/2) - \\ &CQ \times \frac{E_z^n(i, j+1) - E_z^n(i, j)}{\Delta y} \\ H_y^{n+1/2}(i+1/2, j) &= CP \times H_y^{n-1/2}(i+1/2, j) + \\ &CQ \times \frac{E_z^n(i+1, j) - E_z^n(i, j)}{\Delta x} \end{aligned} \quad (3)$$

Where

$$\begin{aligned} CA &= \frac{2\varepsilon(i, j) - \sigma(i, j) \times \Delta t}{2\varepsilon(i, j) + \sigma(i, j) \times \Delta t} \\ CB &= \frac{2\Delta t}{2\varepsilon(i, j) + \sigma(i, j) \times \Delta t} \\ CP &= \frac{2\mu(i, j) - \sigma_m(i, j) \times \Delta t}{2\mu(i, j) + \sigma_m(i, j) \times \Delta t} \\ CQ &= \frac{2\Delta t}{2\mu(i, j) + \sigma_m(i, j) \times \Delta t} \end{aligned} \quad (4)$$

where E_x is the electric field intensity in the direction of the coordinate axis x ; H_x and H_y are the magnetic field intensities in the x and y directions, respectively; Δx and Δy are spatial steps in the x and y directions, respectively; Δt is the time step; n is the step number; and (i, j) is the node coordinate.

To ensure the stable convergence of the solution of the discrete finite-difference equations in the time domain, the time step Δt and spatial steps Δx and Δy are required to satisfy the following relation:

$$\Delta t \leq \frac{1}{c \sqrt{\left(\frac{1}{\Delta x}\right)^2 + \left(\frac{1}{\Delta y}\right)^2}} \quad (5)$$

3.2 Forward modelling scheme

The surrounding rock was assumed to be a continuous, homogeneous medium in a semi-infinite space. The reflection and refraction of electromagnetic waves occurred in two-dimensional planes. The geoelectric model of the plain (left) and reinforced (right) concrete structures was designed (Fig. 1) to study the reflection characteristics of the tunnel lining structure thickness on the GPR forward modelling.

The geoelectric model parameters were set as follows: (1) the area coverage was 3.6 m × 2.4 m, the upper-left corner was the origin of coordinate, the x -coordinate was the horizontal distance, and the y -coordinate was the detection depth; (2) the horizontal distance with a length of 3.6 m was divided into three equal parts, each of them with a length of 1.2 m, and the thickness values were 0.38, 0.33, and 0.28 m from left to right; (3) $\Phi 18$ steel bar, double row layout, the spacing between bars was 0.2 m, and the concrete cover depth was 40 mm; (4) the relative dielectric constant of the concrete lining was six, the conductivity was 0.001 S/m, and the magnetic permeability was 1.

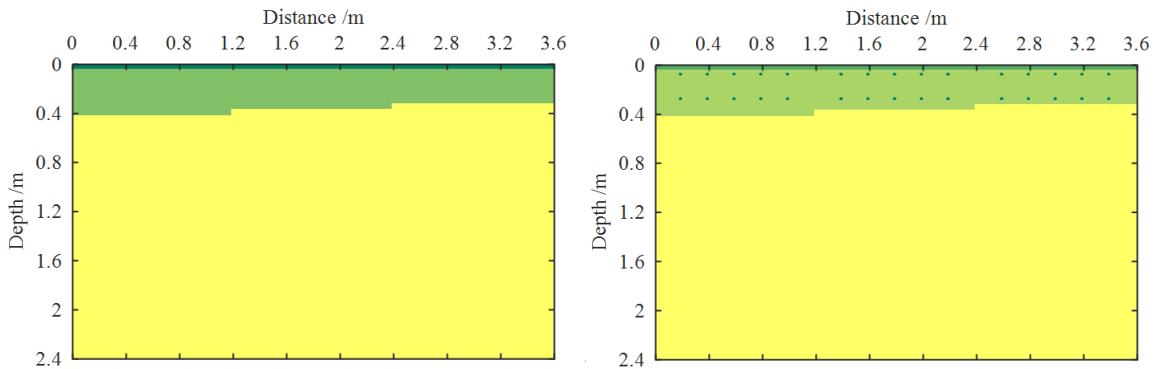


Fig. 1. Geoelectric model of plain (left) and reinforced (right) concrete lining structure

3.3 Radar responses of the lining structure

According to the GPR parameters used in the field detection of tunnel lining structure, the central frequencies of radar antenna utilized in the simulation were 900 and 1600 MHz. The completely matched layers were used as the absorbing boundary conditions. The Ricker wavelet was adopted to simulate the excitation source. The sampling time windows of the 900 and 1600 MHz antennas were 20 and 15 ns, respectively. The space step of the grid was 0.002 m, the

sampling step was 0.01 m, and the number of traces was 340 channels.

GPR antennas of different frequencies were employed to carry out forward modelling for the geoelectric model shown in Fig. 1. The forward modelling radar response images of plain and reinforced concrete could be obtained. On this basis, the algorithms of static correction, subtract-DC-drift, gain, and migration were employed to process the radar response images. The results are shown in Figs. 2 and 3.

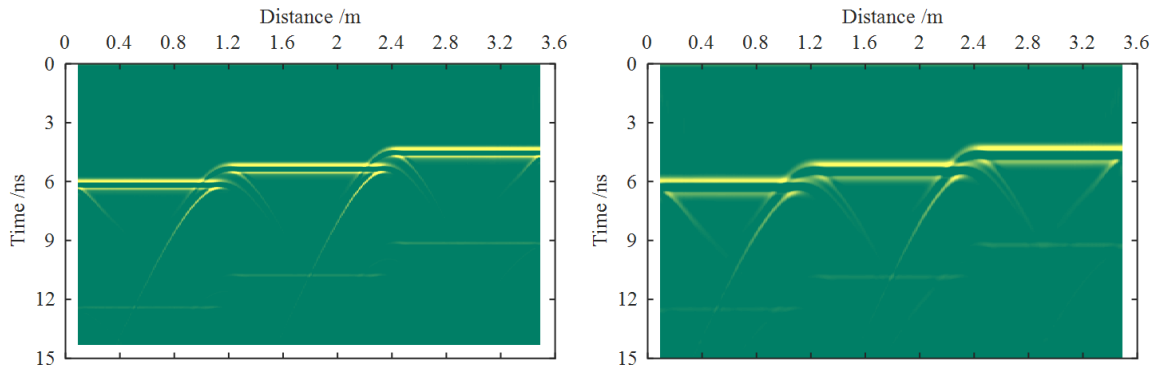


Fig. 2. GPR response of the plain concrete structure with different central frequencies of 1600 (left) and 900 MHz (right)

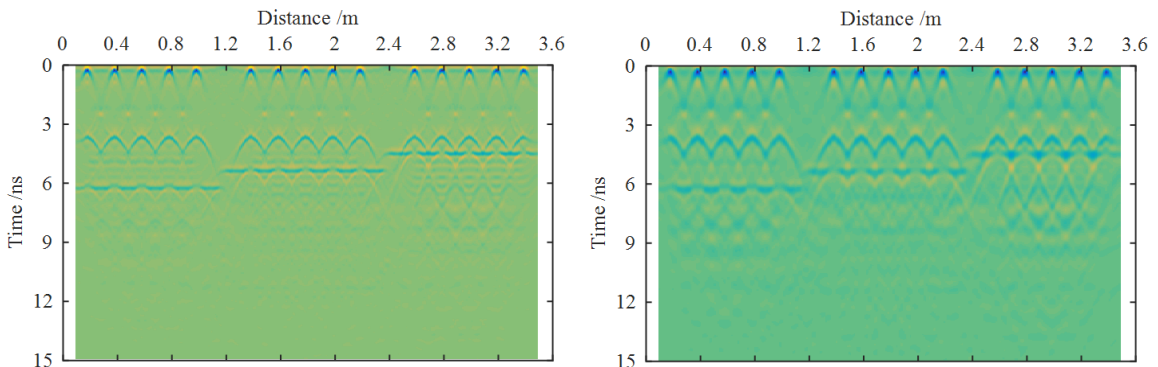


Fig. 3. GPR response of the reinforced concrete structure with different central frequencies of 1600 (left) and 900 MHz (right)

The electromagnetic wave signal was significantly different at the interface due to the difference of the relative dielectric constants between the concrete lining and the surrounding rock. An apparent continuous reflection surface could be seen in the GPR images shown in Figs. 2 and 3. When the thickness of the plain concrete lining suddenly changed, the electromagnetic reflection signal generated a strong diffraction phenomenon. The boundary between the lining structure and the surrounding rock was not obvious because of the strong interference of the steel bar to the electromagnetic wave signal. Specifically, the wavelength of the 1600 MHz antenna was relatively short, which was smaller than the distance between steel bars. The

electromagnetic wave could be transmitted to the interface between the lining structure and the surrounding rock through the distance between steel bars. Therefore, discontinuous radar reflection interface could be found. The wavelength of the 900 MHz antenna was longer than the distance between steel bars. It was difficult for the electromagnetic wave to propagate deep through the distance between steel bars. Therefore, the deep interface was difficult to identify, and other methods were required for further analysis.

3.4 TEDAWT method

The selection of wavelet basis function is not unique in wavelet transform analysis. Different wavelet bases can obtain varying results when the same signal is analyzed. Theoretically speaking, the construction of a new wavelet basis only needs to meet the allowable conditions of wavelet basis. However, the wavelet basis with strong fit between the curve shape and the GPR feature signal can obtain good time–frequency localization analysis effect. According to the features of GPR emission wavelet, pattern adapted waveform matching was carried out by sub-wavelet $f(t) = t^2 e^{-at} \sin \omega_0 t$, and the pattern adapted radar wavelet with high similarity to the GPR sub-wavelet was constructed. The wavelet basis was added to the Wavelet Analysis Toolbox to select the wavelet basis for GPR signal analysis. The multi-scale detailed analysis of the GPR signal could be carried out by using the multi-resolution

characteristic of the wavelet transform. How to select the optimal scale, effectively remove noise and all types of interference signals, and extract meaningful target signals are problems that need to be solved urgently. In the past few years, the time–energy density analysis based on wavelet transform was proposed, thereby successfully avoiding the problem of selecting the optimal scale of the wavelet transform [31–32]. The method provided the energy distribution of the analyzed signal on all scales with time. The wavelet basis for the wavelet transform was constructed by using the above method. The program of the TEDAWT method was written under the working environment of MATLAB language platform. This program was employed to analyze the single-channel signals of typical GPR images with different thicknesses of plain and reinforced concrete lining, as shown in Figs. 2 and 3, respectively. The results are shown in Figs. 4–7.

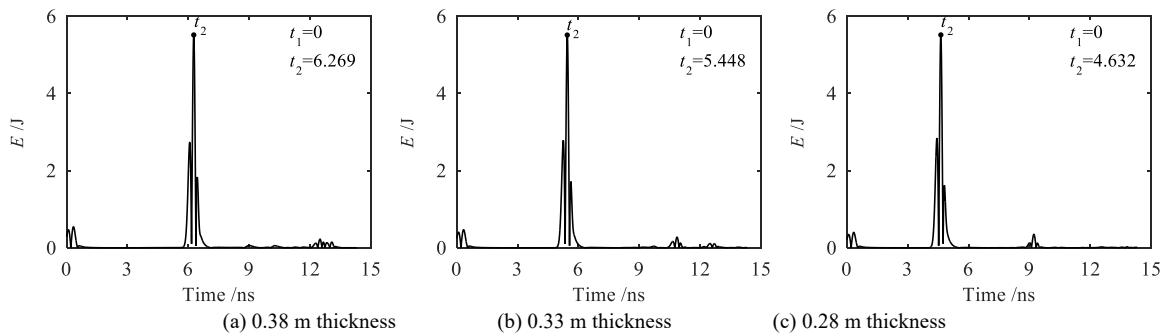


Fig. 4. TEDAWT curve of the single-channel GPR signal in plain concrete forward modelling (1600 MHz)

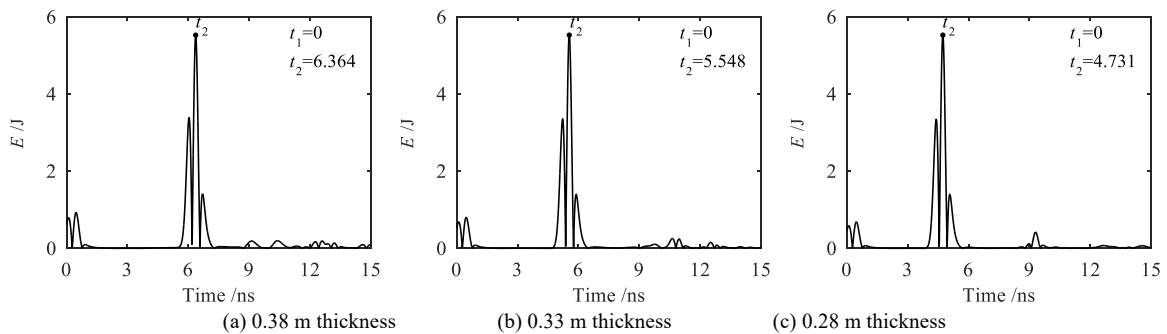


Fig. 5. TEDAWT curve of the single-channel GPR signal in plain concrete forward modelling (900 MHz)

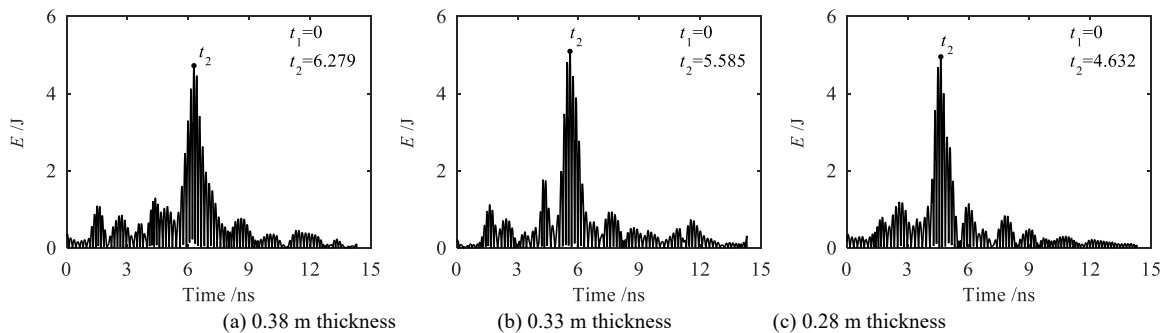


Fig. 6. TEDAWT curve of the single-channel GPR signal in reinforced concrete forward modelling (1600 MHz)

The resolution of the TEDAWT curves of the reinforced concrete shown in Figs. 6 and 7 were lower and exhibited more random disturbances compared with those in Figs. 4 and 5 because of the strong influence of steel bar on electromagnetic wave reflection signal. The TEDAWT curves of single-channel GPR signal in forward modelling had evident peak points because of the plain and reinforced concrete lining structures. The peak point was the reflection position of the electromagnetic wave propagating to the

boundary between the lining structure and the surrounding rock because the direct wave of GPR signal had been removed above. By calculating the round-trip travel time $\Delta t = t_2 - t_1$ on the TEDAWT curves, the thickness L of the concrete lining structure could be obtained by using the formula $L = c \times \Delta t / (2\sqrt{\epsilon})$. In these formulas, the propagation velocity c of the electromagnetic wave in the vacuum is 3.0×10^8 m/ns, t_1 is the reflection position of direct

electromagnetic wave, t_2 is the position of peak point on the TEDAWT curve, and ε is the relative dielectric constant of medium. The forward modelling identification results of the

plain and reinforced concrete lining structures with different thicknesses were summarized, and the results are shown in Table 1.

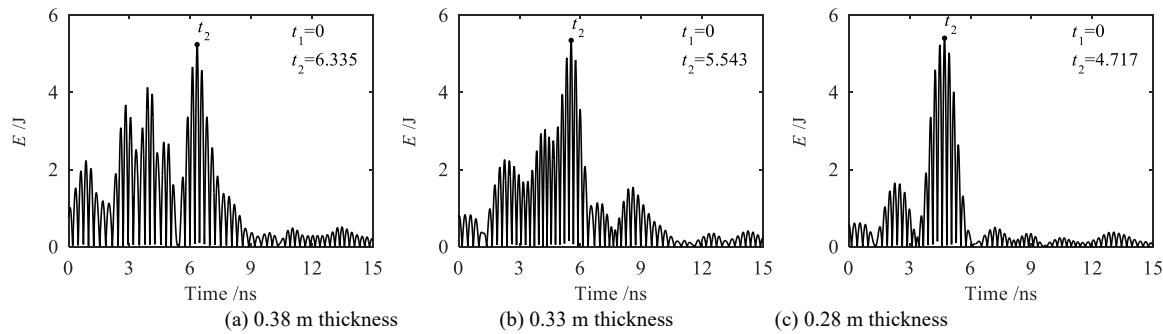


Fig. 7. TEDAWT curve of the single-channel GPR signal in reinforced concrete forward modelling (900 MHz)

Table 1. Identification results and relative errors of forward modelling for the lining structure of different thicknesses

Plain concrete	Lining thickness (cm)			Reinforced concrete	Lining thickness (cm)			Cover depth (cm)
	38	33	28		38	33	28	
1600 MHz	38.39 (1.03%)	33.36 (1.09%)	28.37 (1.12%)	1600 MHz	38.45 (1.18%)	34.20 (3.64%)	28.37 (1.32%)	4.13 (3.25%)
900 MHz	38.97 (2.55%)	33.97 (2.94%)	28.97 (3.46%)	900 MHz	38.79 (2.08%)	33.94 (2.85%)	28.89 (3.18%)	4.91 (22.75%)

Table 1 shows that the wavelength of the 1600 MHz antenna was shorter than that of the 900 MHz antenna. The identified results of concrete lining and cover depth showed higher accuracy than that of the 900 MHz antenna, and the relative error was generally lower. The relative error of lining structure thickness identified by using the TEDAWT method was less than 5% regardless of the 1600 MHz or 900 MHz antenna.

4. Result Analysis and Discussion

4.1 Experimental scheme

Among many scientific research methods, physical experiment has been widely used because of its intuitiveness and reliability. A physical box (4 m × 3 m × 1.5 m size) of

integral casting and molding with different lining thicknesses was created to ensure that the experiment was consistent with the actual condition of the tunnel lining structure. The research focused on the analysis of plain and reinforced concrete structures with three different thicknesses, and their length was 1.2 m. Considering construction errors, such as formwork deformation during pouring, the average thicknesses of each section of the plain concrete measured by the vertical hanging method were 39.58 (Section 1), 34.85 (Section 2), and 29.62 cm (Section 3). Moreover, the average thicknesses of the reinforced concrete were 40.53 (Section 1), 34.48 (Section 2), and 29.83 cm (Section 3). The reinforcement structure consisted of bars with a diameter of 18 mm, spacing of 20 cm, and concrete cover depth of 5.14 cm. Figure 8 shows the specific physical experiment box.

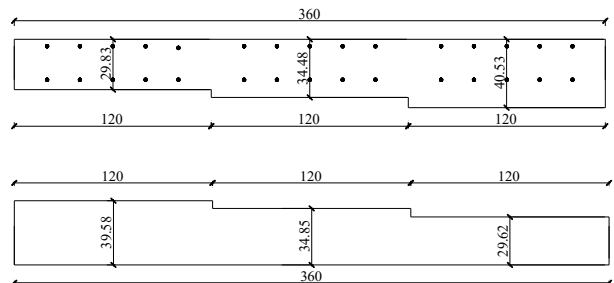


Fig. 8. Physical experiment box of the lining structure with different thicknesses

4.2 GPR data acquisition

The central frequencies of the 1600 and 900 MHz antennas were used for detection to accurately identify the concrete lining structure with different thicknesses. When the same antenna detected the concrete structures of different thicknesses, the GPR parameters remained unchanged.

Because the specific size of the physical experiment box was known, the detection should be conducted from the marked position as the starting point and stop at the marked end position to ensure the integrity of GPR collection. The GPR analysis software was used to perform certain algorithms, such as static correction, subtract-DC-drift, gain, migration,

and band pass filtering on the original signals. The measured

GPR time profiles are shown in Figs. 9 and 10.

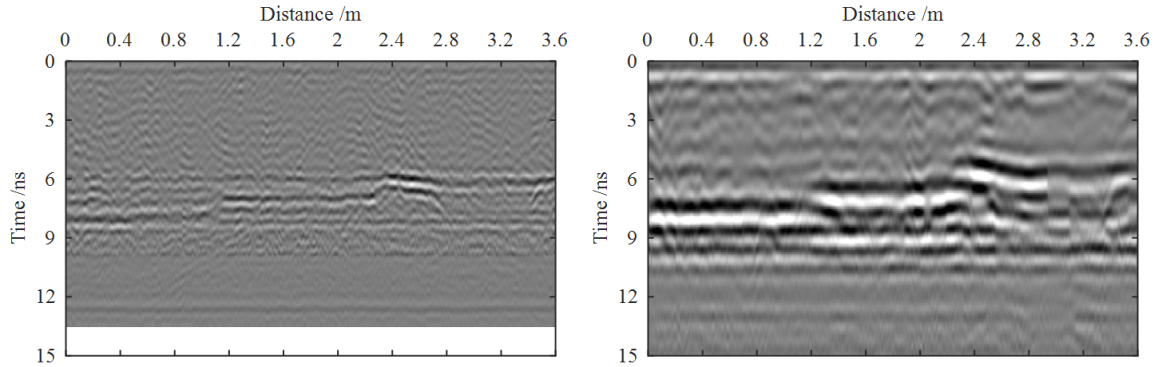


Fig. 9. GPR responses of the plain concrete structure with different central frequencies, namely, 1600 (left) and 900 MHz (right)

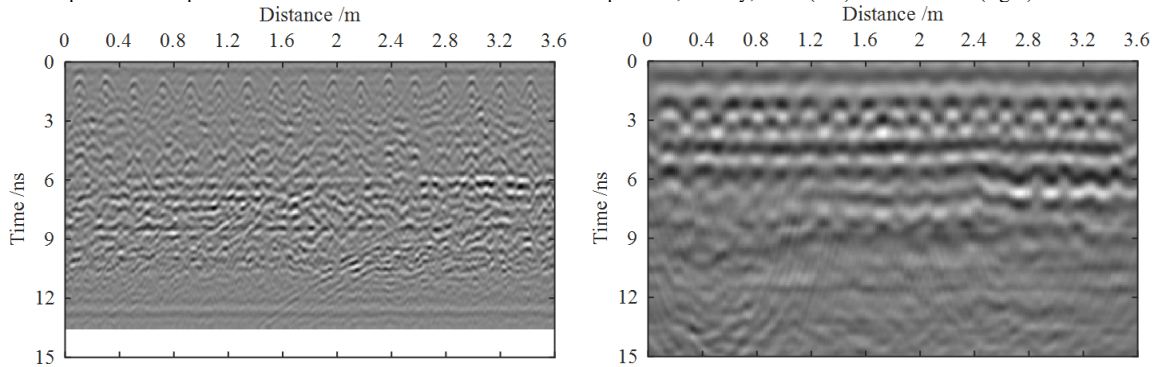


Fig. 10. GPR responses of the reinforced concrete structure with different central frequencies, namely, 1600 (left) and 900 MHz (right)

The measured GPR signals of plain and reinforced concrete with different frequencies had more random noise and lower image resolution compared with the forward modelling images. In either the 1600 or the 900 MHz antenna, the discontinuous dividing lines of different depths could be found on the GPR time profiles with different thicknesses of plain concrete, that is, layer lines of the concrete lining structure with different thicknesses (Fig. 9). In addition, the resolution of the 1600 MHz antenna was higher, and the positioning was more accurate compared with those of the 900 MHz antenna.

As shown in Fig. 10, the first row of steel bars in the concrete lining structure had evident hyperbolic reflection in the GPR image. The strong reflection resulted in fast attenuation of the electromagnetic wave and weak effective signal in deep. The reinforced positioning of the lining structure identified by the 1600 MHz antenna was clearer compared with that of the 900 MHz antenna. That is to say, the concrete cover depth could be clearly identified.

However, the interface between the deep concrete and the surrounding rock were difficult to be identified due to the strong interference of the steel bar to electromagnetic wave reflection. Therefore, the wavelet transform should be used for further analysis.

4.3 Quantitative identification

To accurately obtain the thickness values of different lining structure of reinforced concrete, a single-channel GPR signal was extracted from the time profiles of the measured GPR detection signals of three different thicknesses shown in Figs. 9 and 10. The radar wavelet constructed in Section 3.4 was used as the wavelet basis for the wavelet transform. The program of the TEDAWT method was run in MATLAB language environment. The TEDAWT method was carried out for the single-channel signal of plain and reinforced concrete. The results are shown in Figs. 11–14.

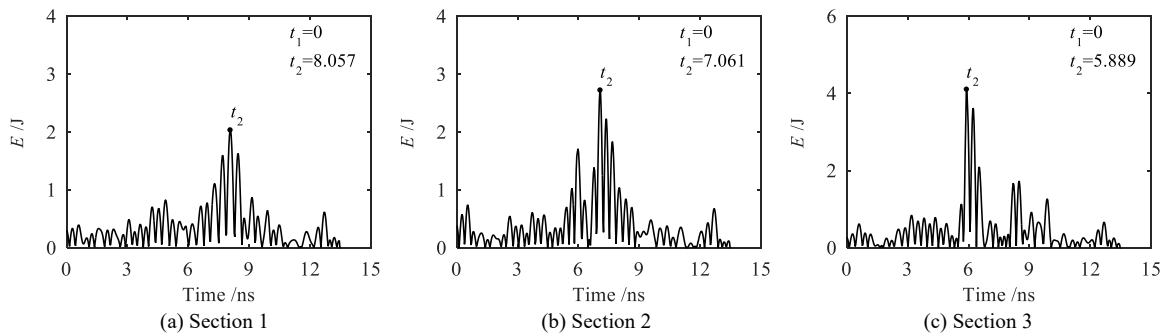


Fig. 11. TEDAWT curve of the single-channel signal in the plain concrete physical experiment (1600 MHz)

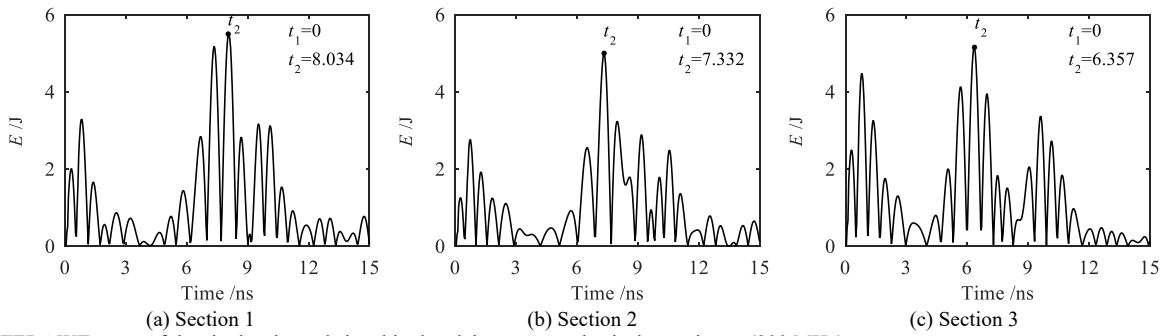


Fig. 12. TEDAWT curve of the single-channel signal in the plain concrete physical experiment (900 MHz)

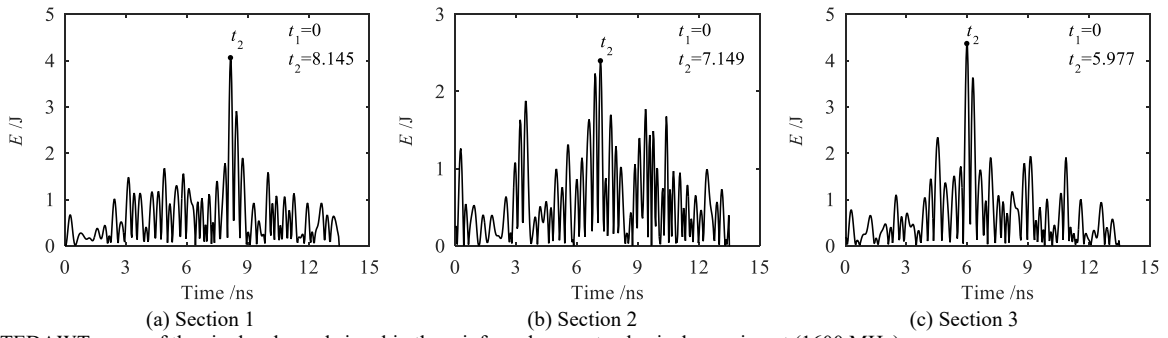


Fig. 13. TEDAWT curve of the single-channel signal in the reinforced concrete physical experiment (1600 MHz)

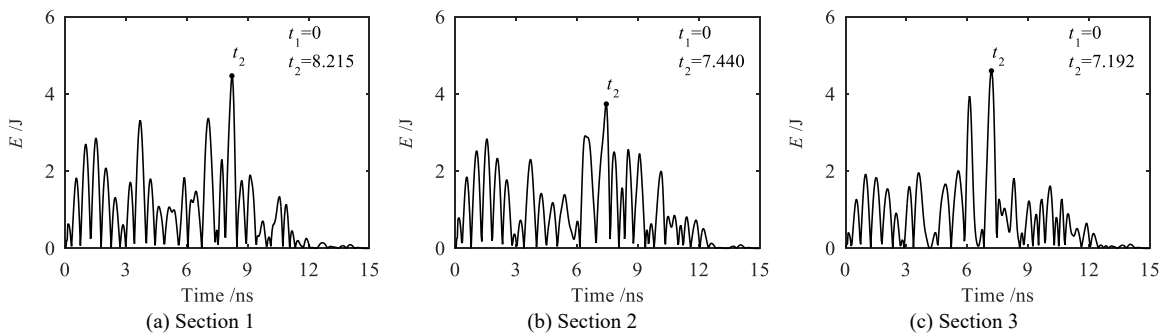


Fig. 14. TEDAWT curve of the single-channel signal in the reinforced concrete physical experiment (900 MHz)

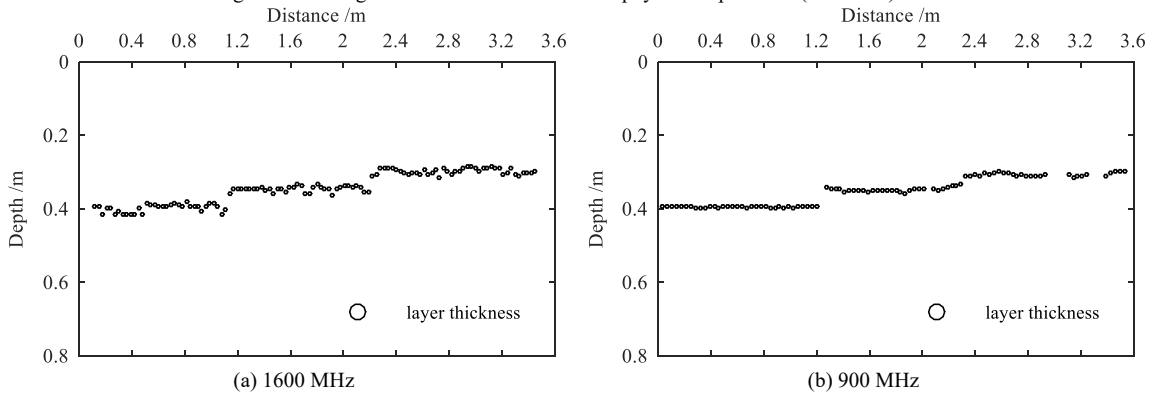


Fig. 15. Identification results of the plain concrete structure with different antenna frequencies

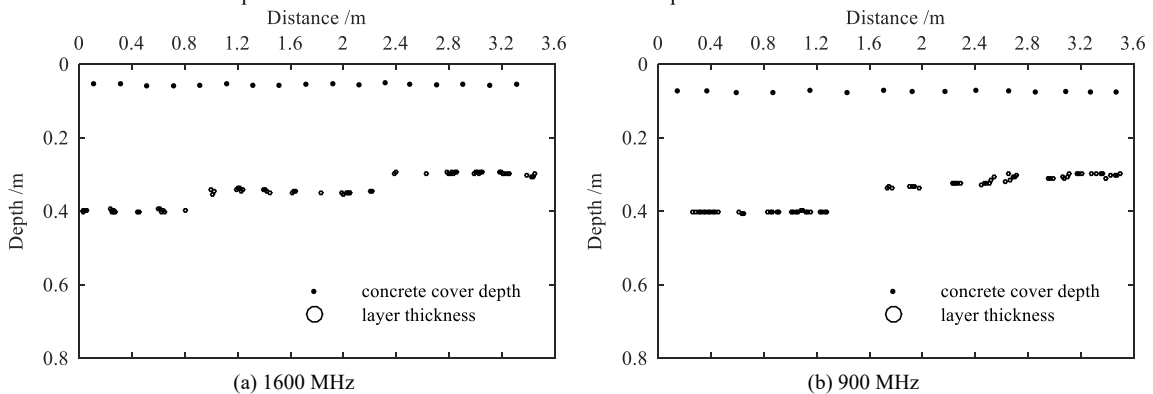


Fig. 16. Identification results of the reinforced concrete structure with different antenna frequencies

Table 2. Identification results and relative errors of the lining thickness for different structures

Plain concrete	Lining thickness (cm)			Reinforced concrete	Lining thickness (cm)			Cover depth (cm)
	39.58	34.85	29.62		40.53	34.48	29.83	
1600 MHz	39.82 (0.61%)	34.60 (0.72%)	29.70 (0.27%)	1600 MHz	39.93 (1.48%)	34.59 (0.32%)	29.65 (0.64%)	4.94 (3.89%)
900 MHz	39.50 (0.23%)	34.74 (0.32%)	30.65 (3.48%)	900 MHz	40.20 (0.81%)	32.85 (1.88%)	30.50 (2.25%)	7.02 (36.6%)

As shown in Figs. 11 to 14, obvious peak points can be observed on the TEDAWT curves of the plain and reinforced concrete detected by different antenna frequencies, that is, the reflection points at the interface between the concrete lining structure and the surrounding rock. Specifically, the positions of the reflection points at the interface of the plain concrete with different thicknesses detected by the 1600 and 900 MHz antenna were 8.057, 7.061, 5.889, 8.034, 7.332, and 6.357 ns. The positions of the reflection points at the interface of the reinforced concrete with different thicknesses detected by the 1600 and 900 MHz antenna were 8.145, 7.149, 5.977, 8.215, 7.440, and 7.192 ns. The thickness value of the concrete lining structure could be obtained by calculating the round-trip travel time on the TEDAWT curve of the single-channel GPR signal. Similarly, the reflection points at the interfaces between the plain or reinforced concrete and the surrounding rock with different thicknesses detected by the 1600 and 900 MHz antenna could be obtained. All reflection points are shown in Figs. 15 and 16.

As shown in Figs. 15 and 16, the layer lines basically reflected the thickness values of the concrete lining at different positions. The 1600 MHz antenna could clearly identify the thickness values of different lining structures of the plain or reinforced concrete compared with the 900 MHz antenna. Table 2 summarizes the identification results of the plain and reinforced concrete lining structures of different thicknesses with various antenna frequencies. The table shows that the thickness values of the plain and reinforced concrete identified by different antenna frequencies were relatively accurate by using the TEDAWT method, and the relative errors were less than 5%. Such results met the needs of practical engineering detection. The 1600 MHz antenna should be preferred for testing the concrete cover depth.

5. Conclusions

To explore the propagation rule of GPR detection signals in the tunnel concrete lining structure, forward modelling and physical experiment were combined together to carry out the non-destructive detection of the lining structure by GPR. The different thicknesses of the plain and reinforced concrete lining were quantitatively identified by using the TEDAWT method. The following conclusions could be drawn:

(1) The feasibility of the TEDAWT method in the identification of different thicknesses of lining structure is verified by GPR forward modelling of plain and reinforced concrete. The method is then applied in the physical experimental test of the plain and reinforced concrete. The results show that the TEDAWT method obtains a good effect in identifying different concrete thicknesses, and the relative error is less than 5%.

(2) The concrete cover depth is an important index of durability of the tunnel concrete lining structure. The 1600 MHz antenna can obtain a higher resolution and smaller relative error whether in the forward modelling or physical experiment compared with the 900 MHz antenna in detecting steel bar images. The 1600 MHz antenna should be used in the actual detection of concrete cover depth as the relative error of the identification results is less than 5%.

(3) The accuracy of identifying the plain and reinforced concrete lining structures and concrete cover depth is high when using the TEDAWT method. This method provides a new feasible approach for the quantitative detection of tunnel lining structure thickness. The TEDAWT method can not only provide the thickness distribution of the plain concrete lining structure but also show the distribution of reinforced concrete lining structure and concrete cover depth compared with traditional GPR profile horizon tracing method.

In the present study, a new method for identifying the different thicknesses of the plain and reinforced concrete lining structures is proposed by combining GPR forward modelling with physical experiment. The reflected characteristics in the method can be used as a reference for the interpretation of the GPR image of the tunnel lining. However, given the lack of field test data, this method should be applied for analysis and processing of field test data in future studies to explain the GPR imaging law of the reinforced concrete lining thickness more accurately.

Acknowledgements

This work was supported by the National Natural Science Foundation of China (Nos. 51608183 and 51678226), the China Scholarship Council (No. 201808430341), and the Natural Science Foundation of Hunan Province in China (No. 2018JJ3022).

This is an Open Access article distributed under the terms of the Creative Commons Attribution License



References

1. Yan J.X., "Achievements and challenges of tunneling technology in China over past 40 years". *Tunnel Construction*, 39(4), 2019, pp. 537-544.
2. Lei J.Q., Ding Z.F., "Development of defect evaluation techniques for highway tunnel lining thickness and compactness". *Modern Tunneling Technology*, 54(4), 2017, pp. 33-40.
3. Zhang Z.Q., Li Y.L., Wang H.Y., Kan C., Li Q., "Effect of steel-bar corrosion on properties of tunnel lining structure". *China Journal of Highway and Transport*, 27(8), 2014, pp. 73-81.
4. Dinh K., Gucunski N., Duong T.H., "An algorithm for automatic localization and detection of rebars from GPR data of concrete bridge decks". *Automation in Construction*, 89, 2018, pp. 292-298.
5. Jiang Y., Wu J.Y., Feng Y., "Study on combined application of geological radar method and shock echo method in defect inspection of railway tunnel lining". *Railway Engineering*, 58(12), 2018, pp. 6-11.
6. Wang Z.C., Wu Y., "A tentative discussion on tunnel lining quality of GPR detection technology". *Geophysical and Geochemical Exploration*, 37(6), 2013, pp. 1152-1156.

7. Zhao C.Y., Deng X.S., "Analysis and approach to the image of the GPR in nondestructive detection of tunnel lining". *Railway Standard Design*, 58(12), 2014, pp. 109-112.
8. Lai W. W. L., Derobert X., Annan P., "A review of ground penetrating radar application in civil engineering: A 30-year journey from locating and testing to imaging and diagnosis". *NDT & E International*, 96, 2018, pp. 58-78.
9. Hasan M. I., Yazdani N., "Ground penetrating radar utilization in exploring inadequate concrete covers in a new bridge deck". *Case Studies in Construction Materials*, 1, 2014, pp. 104-114.
10. Kaur P., Dana K. J., Romero F. A., Gucunski N., "Automated GPR rebar analysis for robotic bridge deck evaluation". *IEEE transactions on cybernetics*, 46(10), 2015, pp. 2265-2276.
11. Li C., Li M.J., Zhao Y.G., Liu H., Wan Z., Xu J.C., Xu X.P., Chen Y., Wang B., "Layer recognition and thickness evaluation of tunnel lining based on ground penetrating radar measurements". *Journal of Applied Geophysics*, 73, 2011, pp. 45-48.
12. Liu Z.H., Wu H., Zhou D., Wei H.Y., "Application of spectrum inversion method in GPR signal processing for tunnel lining detection". *Chinese Journal of Geotechnical Engineering*, 37(4), 2015, pp. 711-717.
13. Shu Z.L., Liu X.R., Liu B.X., Wang D.L., "GPR three-dimensional forward modeling of defects in tunnel lining and engineering verification". *China Railway Science*, 34(4), 2013, pp. 46-53.
14. Kravitz B., Mooney M., Karlovsek J., Danielson I., Hedayat A., "Void detection in two-component annulus grout behind a pre-cast segmental tunnel liner using ground penetrating radar". *Tunnelling and Underground Space Technology*, 83, 2019, pp. 381-392.
15. Giannopoulos A., "Modelling ground penetrating radar by GprMax". *Construction and Building Materials*, 19, 2005, pp. 755-762.
16. Alani A.M., Tosti F., "GPR applications in structural detailing of a major tunnel using different frequency antenna systems". *Construction and Building Materials*, 158, 2018, pp. 1111-1122.
17. Maas C., Schmalzl J., "Using pattern recognition to automatically localize reflection hyperbolas in data from ground penetrating radar". *Computers & Geosciences*, 58, 2013, pp. 116-125.
18. Mechbal Z., Khamlichi A., "Determination of concrete rebars characteristics by enhanced post-processing of GPR scan raw data". *NDT & E International*, 89, 2017, pp. 30-39.
19. Xie X.Y., Qin H., Yu C., Liu L.B., "An automatic recognition algorithm for GPR images of RC structure voids". *Journal of Applied Geophysics*, 99, 2013, pp. 125-134.
20. Jiang Y.J., Zhang X.P., Taniguchi T., "Quantitative condition inspection and assessment of tunnel lining". *Automation in Construction*, 102, 2019, pp. 258-269.
21. Yu Q.M., Zhou H.L., Wang Y.H., Duan R.X., "Quality monitoring of metro grouting behind segment using ground penetrating radar". *Construction and Building Materials*, 110, 2016, pp. 189-200.
22. Llanca D., Breul P., Bacconnet C., "Improving the diagnosis methodology for masonry tunnels". *Tunnelling and Underground Space Technology*, 70, 2017, pp. 55-64.
23. Xiang L., Zhou H.L., Shu Z., Tan S.H., Liang G.Q., Zhu J., "GPR evaluation of the Damaoshan highway tunnel: A case study". *NDT & E International*, 59, 2013, pp. 68-76.
24. Zan Y. W., Li Z. L., Su G. F., Zhang Y. Y., "An innovative vehicle-mounted GPR technique for fast and efficient monitoring of tunnel lining structural conditions". *Case Studies in Nondestructive Testing and Evaluation*, 6, 2016, pp. 63-69.
25. Cui Y., Wang L., Xiao J., "Automatic feature recognition for GPR image processing". *World Academy of Science, Engineering and Technology*, 61, 2010, pp. 176-179.
26. Baryshnikov V. D., Khmelin A. P., Denisova E. V., "GPR detection of inhomogeneities in concrete lining of underground tunnels". *Journal of Mining Science*, 50(1), 2014, pp. 25-32.
27. Lalagüe A., Lebens M. A., Hoff L., GrØv E., "Detection of rockfall on a tunnel concrete lining with ground-penetrating radar (GPR)". *Rock Mechanics and Rock Engineering*, 49(7), 2016, pp. 2811-2823.
28. Zhang D.L., Zhang S.L., Fang Q., Chen F.B., "Study of contact state behind tunnel lining in process of railway operation and its analysis". *Chinese Journal of Rock Mechanics and Engineering*, 32(2), 2013, pp. 217-224.
29. Li Y., Li S.C., X. L., Liu B., Lin C.J., Z F.K., Y L., "Forward simulation of ground penetrating radar and its application to detection of tunnel lining diseases". *Rock and Soil Mechanics*, 237(12), 2016, pp. 3627-3634.
30. Lv G., Li N., Liu X.X., Zhu C.H., "FDTD forward modeling of geometric shape and fillings of lining defects of highway tunnel". *Chinese Journal of Rock Mechanics and Engineering*, 33(7), 2014, pp. 1415-1423.
31. Yan P., Lu W.B., Luo Y., Zhou C.B., "Identification of arriving time of vibration induced by geostress dynamic unloading during blasting-excavation employing method of time-energy analysis based on wavelet transform". *Chinese Journal of Rock Mechanics and Engineering*, 28(S1), 2009, pp.2836-2844.
32. Zhang S., Ling T.H., Liu H.R., Cao F., "Pattern adapted wavelet time-energy density method and its application in millisecond blast vibration signal analysis". *Journal of the China Coal Society*, 39(10), 2014, pp. 2007-2013.